Passive longitudinal phase space linearizer

P. Craievich

Sincrotrone Trieste–ELETTRA, Trieste, Italy

(Received 23 September 2008; published 30 March 2010)

We report on the possibility to passively linearize the bunch compression process in electron linacs for the next generation x-ray free electron lasers. This can be done by using the monopole wakefields in a dielectric-lined waveguide. The optimum longitudinal voltage loss over the length of the bunch is calculated in order to compensate both the second-order rf time curvature and the second-order momentum compaction terms. Thus, the longitudinal phase space after the compression process is linearized up to a fourth-order term introduced by the convolution between the bunch and the monopole wake function.

DOI: 10.1103/PhysRevSTAB.13.034401 PACS numbers: 41.20.−q, 29.27.−a, 41.60.−m

I. INTRODUCTION

In an x-ray free electron laser (FEL), the electron bunch is usually compressed to increase the peak current [1] and thus increase the overall efficiency. This compression process is strongly affected by nonlinear effects such as the sinusoidal rf time curvature and the second-order path-length dependence on particle energy in the magnetic chicane. In [2] and references contained therein, it is proposed to use a short section of radio-frequency accelerating fields at a higher harmonic with respect to the main accelerating linac to linearize the longitudinal phase space of the overall compression process. This technique linearizes the compression transformation through second order. In this note we describe the use of a passive dielectric-lined waveguide to linearize the longitudinal phase space through the compression process instead of an active higher harmonic system. But use of the passive linearizer is not perfect and, after the convolution with the charge distribution, it introduces a fourth-order term in the position-energy behavior that changes the initial bunch profile.

In Sec. II and using the concepts presented in [3], we summarize the longitudinal single-mode wakes in a dielectric-lined waveguide considering only the two first characteristic waves. In Sec. III we give an explicit expression for the energy change within a rectangular bunch distribution upon passage through a dielectric-lined waveguide when only the first characteristic wave is considered for the wake function. Thus, as suggested in [2], we work out the voltage needed to completely cancel the second-order compression factor. Furthermore, we give a condition to limit the residual nonlinear effects due to the fourth-order term introduced by the convolution between the bunch distribution and the induced wake function of the linearizer. In Sec. IV we present the tracking results considering two cases for a rectangular bunch distribution and the linear compression factor. It is worthwhile noting that the energy change within the bunch due to passage through the dielectric-lined waveguide strongly depends on the charge and bunch distribution. For this reason we also look at the sensitivity of the process as a function of the bunch distribution, in particular the bunch length, and charge variations. In Sec. V we consider a linear ramped bunch distribution such as that used in [1] and, as in the previous section, we work out the voltage needed to cancel the second-order compression terms. For this case we also give a condition to limit the residual nonlinear effects. In Sec. VI we present the tracking results when a passive linearizer is used together with an active fourth-harmonic system in the one-stage compression option of the FERMI@Elettra project [4].

II. LONGITUDINAL WAKE FUNCTION

Following [3], we summarize in this section relevant aspects of the longitudinal single-mode wakes generated in a dielectric-lined waveguide via passage of a charged particle. Let us consider a charged particle traveling with a speed close to that of light through a pipe of circular cross section and radius r_2. Let us also assume that the wall of the pipe have infinite conductivity and that it is lined with dielectric material between radii $r_1 < r < r_2$. In the case of such a dielectric-lined waveguide, the longitudinal wake function for the monopole mode, considering only the two first characteristic waves, is

$$w_{||}(z) \approx A_0 \cos(k_s z) + A_1 \cos(k_{s1} z), \tag{1}$$

where the amplitudes are

$$A_0 = \frac{Z_0 c}{4\pi} \frac{1}{r_2^2} \frac{4}{\epsilon\xi} \frac{x_0 p_0(x_0)}{(d/dx) D_0(x_0)} \tag{2}$$

$$A_1 = \frac{Z_0 c}{4\pi} \frac{1}{r_2^2} \frac{4}{\epsilon\xi} \frac{x_1 p_0(x_1)}{(d/dx) D_0(x_1)}, \tag{3}$$

where Z_0 is the impedance of free space, $\xi = r_1/r_2$, and ϵ

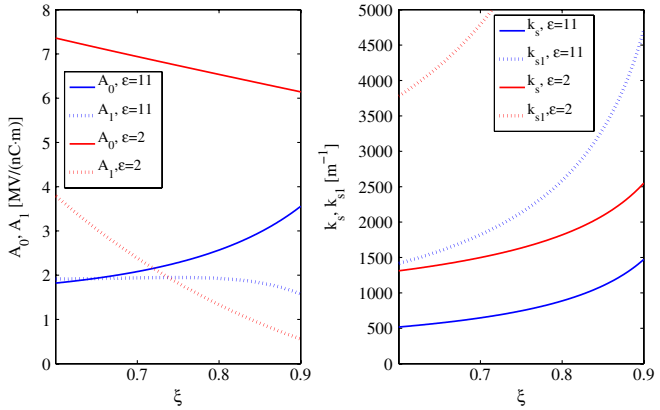

FIG. 1. (Color) Amplitudes (A_0 and A_1) and wave numbers (k_s and k_{s1}) as a function of the parameter $\xi = r_1/r_2$ for $r_2 = 2.5$ mm.

is the relative permittivity. The wave numbers of the characteristic waves are defined by

$$k_s = \frac{x_0}{r_2\sqrt{\epsilon - 1}} \tag{4}$$

$$k_{s1} = \frac{x_1}{r_2\sqrt{\epsilon - 1}}, \tag{5}$$

where x_0 and x_1 are the first two positive zeros of the analytical function:

$$D_0(x) = xp_0'(x) + \frac{x^2\xi}{2\epsilon}p_0(x) \tag{6}$$

with

$$p_0(x) = J_0(x)Y_0(\xi x) - J_0(\xi x)Y_0(x) \tag{7}$$

$$p_0'(x) = J_0(x)Y_0'(\xi x) - J_0'(\xi x)Y_0(x) \tag{8}$$

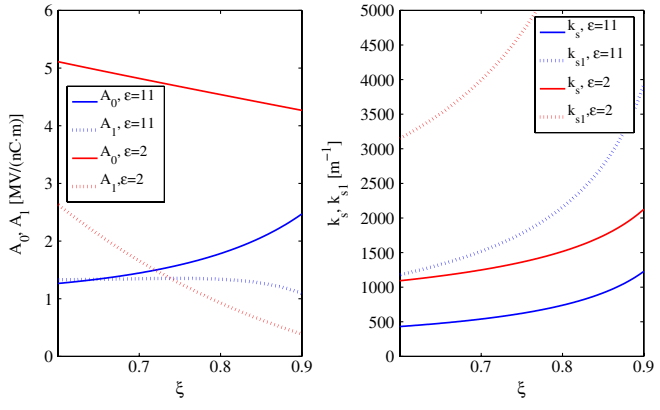

FIG. 2. (Color) Amplitudes (A_0 and A_1) and wave numbers (k_s and k_{s1}) as a function of the parameter $\xi = r_1/r_2$ for $r_2 = 3$ mm.

and where J_0 and Y_0 are, respectively, the Bessel function of order zero and the Neumann function of order zero.

We assume that the higher-order modes of wave numbers k_{sn} are suppressed due to the practical consideration that there will be a finite rms bunch length σ. However, in Sec. VI we give the particle tracking result when the second characteristic wave of wave number k_{s1} is also considered. Figures 1 and 2 show the amplitudes and wave numbers of the two first characteristic waves as a function of the parameter ξ for $r_2 = 2.5$ mm and $r_2 = 3$ mm, respectively.

III. RECTANGULAR BUNCH DISTRIBUTION

For a rectangular bunch distribution $\rho_R(z)$ with full-width L_b, total charge Q, and distributed symmetrically about $z = 0$, the energy change within the bunch due to its passage through a dielectric-loaded vacuum chamber of length L and subject to the wake of the first characteristic monopole mode is given by

$$\begin{aligned}\Delta E_s(z) &= -eQL\int_{-\infty}^{z} w_{||}(z - z')\rho_R(z')dz' \\ &= \begin{cases} -eQLA_0\frac{\sin(\frac{k_sL_b}{2})}{\frac{k_sL_b}{2}}\cos(k_sz) & \text{if } z > \frac{L_b}{2}, \\ -\frac{eQLA_0}{k_sL_b}\sin(k_sz + \frac{k_sL_b}{2}) & \text{if } |z| \le \frac{L_b}{2}, \\ 0 & \text{if } z < -\frac{L_b}{2}. \end{cases}\end{aligned} \tag{9}$$

Let us consider that the electron beam passes through one linac segment and then through a round pipe partially filled with dielectric material as described above. If the beam has an initial mean energy E_i, then following the linac and after the round pipe the electron energy for particles with $|z_0| \le L_b/2$ is

$$E(z_0) = E_i + eV_1\cos(k_1z_0 + \phi_1) - eA_s\sin(k_sz_0 + \phi_s), \tag{10}$$

where k_1 is the rf wave number, V_1 is the amplitude of the voltage of the linac segment, z_0 is the longitudinal position of the particle with respect to the bunch center, and the bunch head is at $z_0 < 0$, $A_s = (QLA_0)/(k_sL_b)$, and $\phi_s = (k_sL_b)/2$. The rf phase ϕ_1 is defined to be zero at accelerating crest and a phase in the interval $-90° < \phi_1 < 0$ will accelerate the bunch head less than the bunch tail.

The synchronous mode can provide a decelerating voltage at the bunch center when its phase is $\phi_s \sim \pi/2$ and this condition can be obtained by choosing a dielectric-lined waveguide with $k_s \sim \pi/L_b$. The relative energy deviation can be expanded in a power series about the reference particle and becomes

$$\frac{\Delta E(z_0)}{E_0} \approx -\frac{eV_1k_1\sin(\phi_1)+eA_sk_s\cos(\phi_s)}{E_0}z_0 - \frac{eV_1k_1^2\cos(\phi_1)-eA_sk_s^2\sin(\phi_s)}{2E_0}z_0^2 + \frac{eA_sk_s^3\cos(\phi_s)}{6E_0}z_0^3 - \frac{eA_sk_s^4\sin(\phi_s)}{24E_0}z_0^4, \quad (11)$$

where E_0 is the chicane energy. In Eq. (11) we choose to expand up to the fourth order in bunch length coordinate z_0 for the energy change due to the dielectric-loaded vacuum chamber, while assuming that $k_1L_b \ll 1$ we choose to expand only up to the second order in bunch length for the energy gain from the linac. Let us write the relative energy deviation in (11) as

$$\frac{\Delta E}{E_0} \approx az_0 + bz_0^2 + cz_0^3 + dz_0^4. \quad (12)$$

A magnetic chicane is next used to transform energy deviations into path-length deviations. The chicane transformation can be written to third order in relative energy deviation as

$$z = z_0 + R_{56}\frac{\Delta E}{E_0} + T_{566}\left(\frac{\Delta E}{E_0}\right)^2 + U_{5666}\left(\frac{\Delta E}{E_0}\right)^3, \quad (13)$$

where $T_{566} \approx -3R_{56}/2$ and $U_{5666} \approx 2R_{56}$ for a typical chicane, and R_{56}, T_{566}, and U_{5666} are the linear, second-order, and third-order transport matrix elements relating energy offset to longitudinal displacements following transport through the chicane. Putting Eq. (12) into Eq. (13) we obtain

$$z = (1+aR_{56})z_0 + (bR_{56}+a^2T_{566})z_0^2 + (2abT_{566}+a^3U_{5666}+R_{56}c)z_0^3 + (dR_{56}+b^2T_{566}+3a^2bU_{5666}+2caT_{566})z_0^4 + (3U_{5666}ca^2+3U_{5666}ab^2+2T_{566}da+2T_{566}cb)z_0^5 + (3U_{5666}da^2+6U_{5666}abc+Ub^3+2T_{566}db+T_{566}c^2)z_0^6 + (3U_{5666}b^2c+6U_{5666}adb+3U_{5666}ac_2^2T_{566}dc)z_0^7 + (3U_{5666}b^2d+3U_{5666}bc^2+6U_{5666}acd+T_{566}d^2)z_0^8 + (U_{5666}c^3+6U_{5666}bcd+3U_{5666}ad^2)z_0^9 + (3U_{5666}c^2d+3U_{5666}bd^2)z_0^{10} + (3U_{5666}cd^2)z_0^{11} + (U_{5666}d^3)z_0^{12}. \quad (14)$$

Fixing $k_1z_0 \ll 1 \quad \forall\ z_0$, $k_1 \ll k_s$, $\phi_s \sim \pi/2$, $eV_1 \sim E_0$, $QLA_0 \ll E_0$, and $k_s \sim \pi/L_b$, an order analysis is performed and Eq. (14) can be simplified as

$$z \approx (1+aR_{56})z_0 + (bR_{56}+a^2T_{566})z_0^2 + dR_{56}z_0^4. \quad (15)$$

In order to evaluate the quality of the analytical treatment and the degree of confidence in the assumption concerning the approximations, we perform a comparison between the results obtained with Eq. (13) without approximations and how this deviates from the approximation of Eq. (15). For this purpose, we consider a realistic set of parameters reported in Table I and also used in the following paragraphs. These parameters are close to the design parameters of the FERMI@Elettra project [1]. Figure 3 shows that there is very good agreement between the two results.

TABLE I. The rf and bunch compression parameters for the second-order compensation with the passive linearizer ($C = 3.5$).

Parameter	
V_1	150.3 MV
ϕ_1	−26.1 deg
R_{56}	−3.95 cm
A_s	0.94 MV
$n = k_s/k_1$	14.33
r_1	2.48 mm
r_2	3.50 mm
ϵ	2.8
A_0	2.95 MV/(nC m)
L_{guide}	1 m

To compensate the quadratic term in the transformation in Eq. (15), the second term must be set to zero:

$$bR_{56} + a^2T_{566} = 0, \quad (16)$$

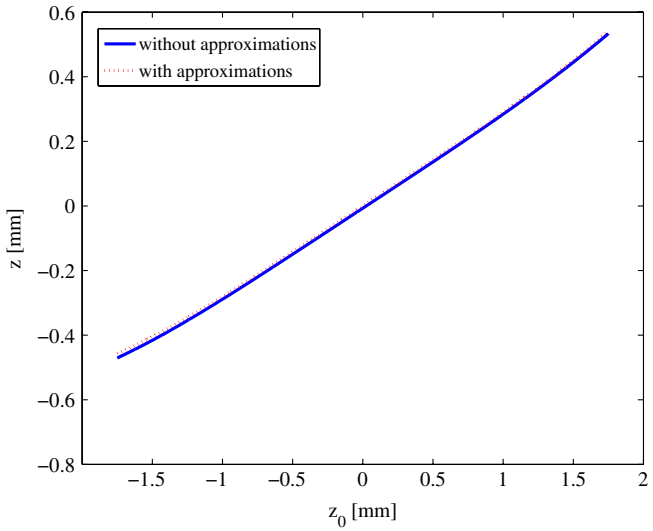

FIG. 3. (Color) Comparison between the compression obtained numerically in Eq. (13) without the approximations and the compression given by Eq. (15), i.e., derived from the approximation in the power series for the energy variation of Eq. (12) and from the simplification due to the order analysis of Eq. (14).

that is,

$$b = -\frac{T_{566}}{R_{56}}a^2 \approx \frac{3}{2}a^2. \tag{17}$$

Choosing to hold the energy at the chicane constant and at E_0 and assuming that the synchronous mode is decelerating, then it is necessary to increase the voltage of the linac:

$$eV_1\cos(\phi_1) = E_0 - E_i + eA_s\sin(\phi_s). \tag{18}$$

A second requirement is to hold the compression factor, $C = 1/(1 + aR_{56})$, constant. If the R_{56} is fixed, then the requirement is to hold the parameter a constant:

$$eV_1\sin(\phi_1) = -\frac{aE_0}{k_1} + eA_s\frac{k_s}{k_1}\cos(\phi_s). \tag{19}$$

Using (18) to eliminate the eV_1 terms from Eq. (17), we can calculate the amplitude of the voltage A_s needed to completely cancel the second-order compression terms:

$$eA_s = \frac{1}{\sin(\phi_s)}\frac{E_0(1+\frac{3a^2}{k_1^2}) - E_i}{(\frac{k_s}{k_1})^2 - 1}. \tag{20}$$

If $k_s \gg k_1$ and $\sin(\phi_s) \sim 1$ then the amplitude A_0 of the synchronous mode can be written

$$A_0 \approx \frac{L_b}{k_s}\frac{k_1^2 A_{s0}}{QL}, \tag{21}$$

where

$$eA_{s0} = E_0\left(1 + \frac{3a^2}{k_1^2}\right) - E_i. \tag{22}$$

In Eq. (15) the residual nonlinear effects are small if the fourth-order term is maintained small compared with the linear compression term, that is,

$$1 + aR_{56} \gg dR_{56}\left(\frac{L_b}{2}\right)^3 \tag{23}$$

considering the worst condition at the tail of the bunch where $z_0 = L_b/2$. The condition (23) can be rearranged as follows:

$$\left|\frac{R_{56}}{1 + aR_{56}}\right| \ll \frac{192E_0}{\pi^2 k_1^2 eA_{s0}L_b}. \tag{24}$$

Here we have assumed $k_s L_b \sim \pi$ and $\sin(\phi_s) \sim 1$. Basically, there are two possibilities to limit the residual nonlinear effects: the first one is to reduce the bunch length L_b from the photoinjector and the second one is to limit the linear compression factor $C = 1/(1 + aR_{56})$. When the charge and the length of the electron bunch are fixed, we can choose a dielectric- lined vacuum chamber with $k_s \sim \pi/L_b$ and A_0 from Eq. (21). In order to accommodate a range of bunch charges and current distributions, one possible idea would be implement a set of passive linearizers on a movable stage. Each linearizer would be "tuned" to different values of k_s and A_0 and so could be used for a range of bunch length and charge. Another possible idea would be to use a parallel plate waveguide configuration where changing the gap could be used to vary the synchronous mode.

In the following paragraphs, we present the results from the tracking analysis considering two bunch length cases both with a total charge of 1 nC. For both cases we also consider relative bunch length and relative charge variations up to 20% with respect to the nominal parameters at the injector in order to gauge the method's sensitivity to fluctuations.

IV. TRACKING RESULTS FOR A RECTANGULAR BUNCH DISTRIBUTION

In this section we present the LITRACK [5] tracking results for two bunch length cases, $L_b = 3.5$ mm and $L_b = 2$ mm. In the former case the linear compression factor is limited to $C = 3.5$, while in the latter the linear compression factor is limited to $C = 6$. The nominal energy at the chicane is $E_0 = 230$ MeV, while the initial energy is $E_i = 96$ MeV. The wave number of the main accelerating linac is $k_1 = 62.9$ m^{-1}. A rectangular bunch distribution with total charge $Q = 1$ nC is used for both cases.

A. Case 1: $L_b = 3.5$ mm and $C = 3.5$

Figure 4 shows the simulated energy profile, longitudinal phase space, and bunch current distribution after the bunch compressor chicane without second-order compensation ($V_1 = 149.4$ MeV, $\phi_1 = -26.3$ deg, and $R_{56} = -3.95$ cm). A current spike develops at the bunch head due to the combined rf and compression nonlinearities.

Figure 5 shows the phase space and the bunch current distribution after the bunch compressor chicane when an active fourth-harmonic rf system is used to compensate the quadratic term introduced by the accelerating rf system and the compressor (in this case the harmonic voltage is -12.7 MV while $V_1 = 161.0$ MeV, $\phi_1 = -24.3$ deg, and $R_{56} = -3.95$ cm). The compressed current distribution is nearly unchanged with respect to the initial profile (i.e. it is still rectangular) and the energy-z correlation is linear.

Table I lists the rf and bunch compression parameters when a passive linearizer is used. The harmonic voltage A_s was calculated from Eq. (20) and $k_s = \pi/L_b \approx 890$ m^{-1}. The voltage and phase of the linac were adjusted in order to be used with the passive linearizer. Figure 6 shows the phase space after the chicane when the passive linearizer is used to compensate the quadratic term. If the remaining fourth-order term remains limited, then the phase space is quite linear and the current distribution does not develop a significant sharp current spike at the head of the bunch. On the other hand, there is a distortion of the current distribution due to the fourth-order term introduced by the passive linearizer. Table I lists parameters for a possible dielectric-

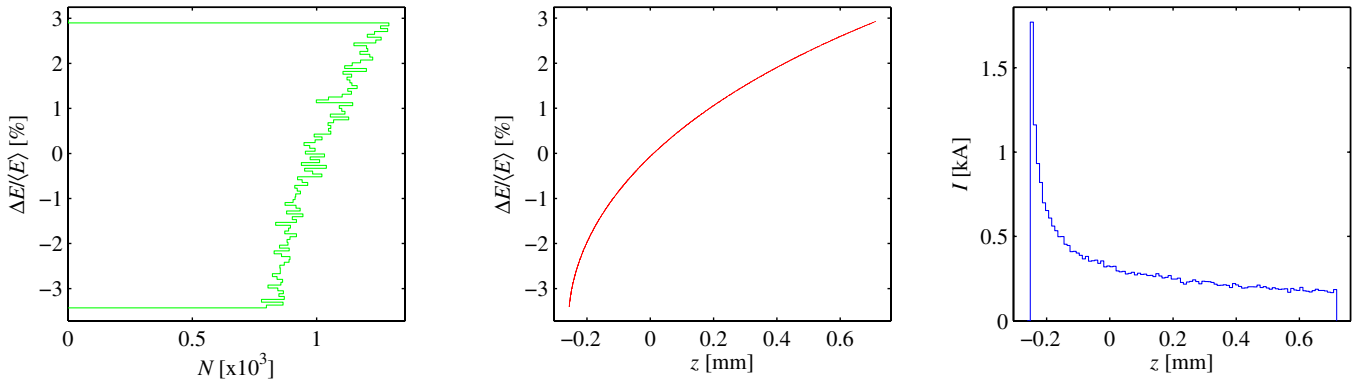

FIG. 4. (Color) Energy profile (left), longitudinal phase space (middle), and beam current distribution (right) after the bunch compressor chicane without passive linearizer or active fourth-harmonic system. An undesirable sharp current spike develops at the bunch head due to the quadratic term in the rf followed by the chicane compression. Bunch head at left, $z < 0$.

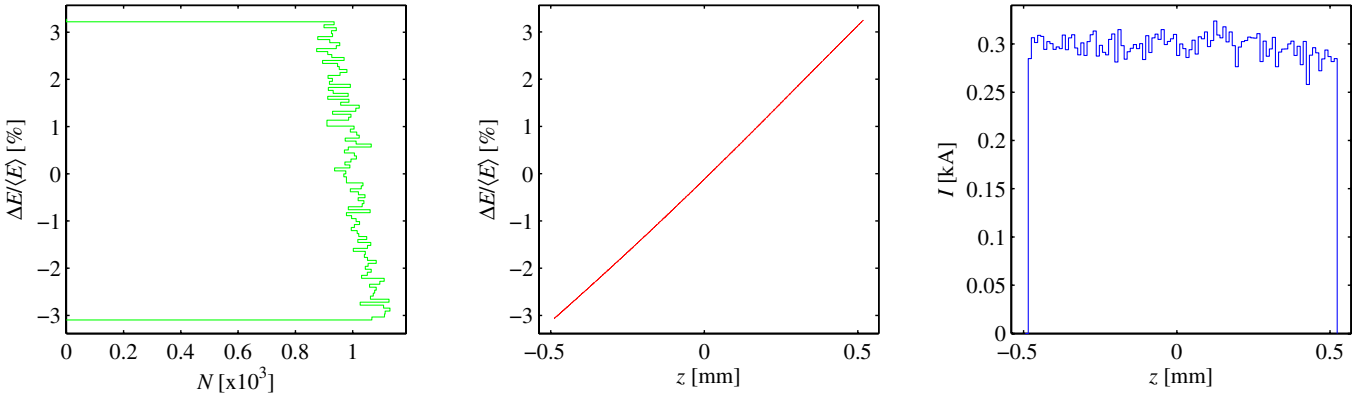

FIG. 5. (Color) Energy profile (left), longitudinal phase space (middle), and bunch current distribution (right) after the chicane when a fourth-harmonic rf system (x band) is used.

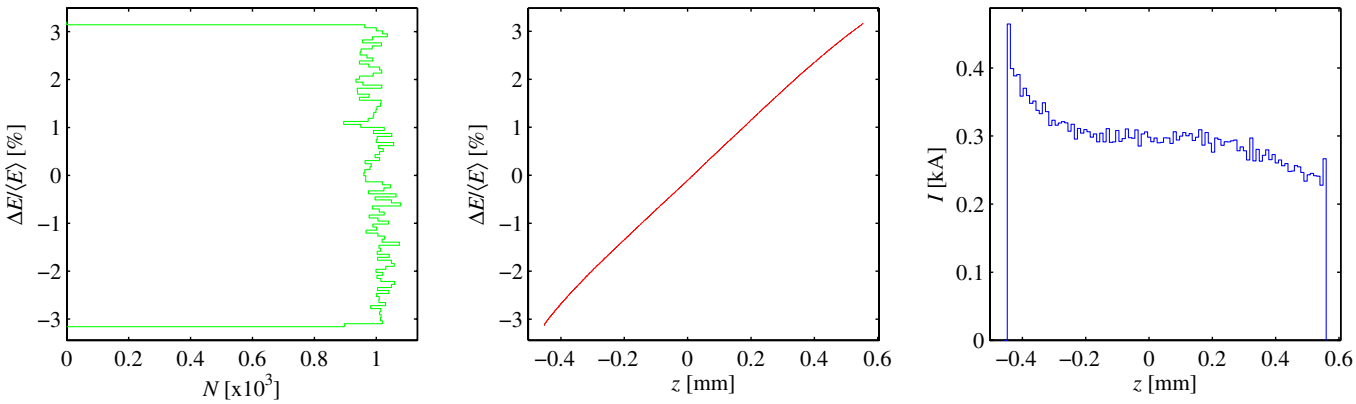

FIG. 6. (Color) Energy profile (left), longitudinal phase space (middle), and bunch current distribution (right) after the chicane when the passive linearizer is used to compensate the quadratic term. The goal is to have the compression factor $C = 3.5$.

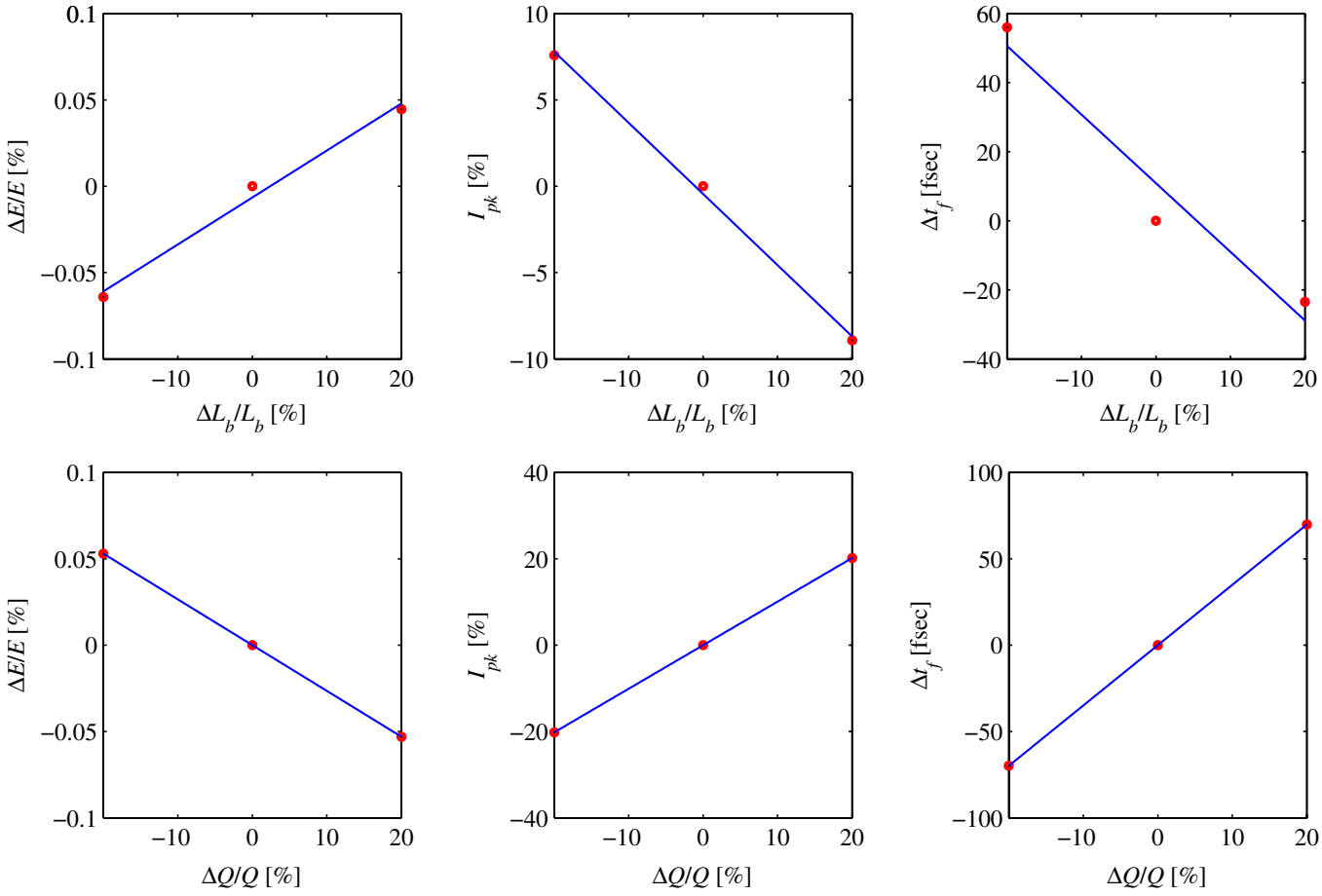

FIG. 7. (Color) Relative mean energy $\Delta E/E$, relative peak current $\Delta I_{pk}/I_{pk}$, and bunch arrival time variations Δt_f as a function of the relative initial bunch length variations $\Delta L_b/L_b$ (upper plots) and relative initial bunch charge variations $\Delta Q/Q$ (lower plots).

lined waveguide that would meet the requirements necessary to produce the results of Fig. 6. This dielectric-lined waveguide would have radii $r_1 = 2.48$ mm and $r_2 = 3.5$ mm, would be 1-m long, and would be lined with a dielectric material with $\epsilon = 2.8$.

We next look at the sensitivity of the process as a function of the bunch length and charge variations. Figure 7 plots the relative peak current $\Delta I_{pk}/I_{pk}$, relative mean energy $\Delta E/E$, and bunch arrival time variation Δt_f after the bunch compression as a function of the bunch length variation $\Delta L_b/L_b$ (upper plots) and the relative charge variations $\Delta Q/Q$ (lower plots) at the injector. As an example, the upper middle plot in Fig. 7 indicates that a $\pm 19\%$ bunch length variation at the injector causes an approximately to $\mp 8\%$ relative peak current variation after the bunch compression. Table II lists the sensitivities of the electron beam parameters to the relative bunch length and charge variations. Each sensitivity number quoted in the table independently causes an 8% relative peak current increase, a 0.1% relative mean energy increase, and a 150 fs bunch arrival time increase. Figure 8 shows the bunch current distributions after the bunch compression chicane for different bunch length variations at the injector and for different relative bunch charge variations. We can

TABLE II. Individual sensitivities. Each parameter variation causes a $\Delta I_{pk}/I_{pk} = +8\%$ relative peak current change, or a $\Delta E/E_0 = +0.1\%$ relative energy change or a $\Delta t_f = 150$ fs bunch arrival time change after the bunch compression.

Parameters	$\Delta I_{pk}/I_{pk} = +8\%$	$\Delta E/E = +0.1\%$	$\Delta t_f = +150$ fs
$\Delta L_b/L_b$ [%]	-19	>20	< -20
$\Delta Q/Q$ [%]	8	< -20	>20

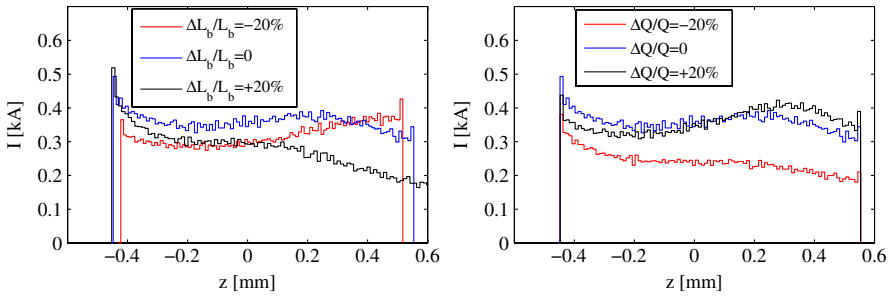

FIG. 8. (Color) Bunch current distributions after the chicane for different bunch length variations at the injector (left plot) and for different relative bunch charge variations (right plot).

TABLE III. The rf and bunch compression parameters for the second-order compensation with the passive linearizer ($C = 6$).

Parameter	
V_1	149.5 MV
ϕ_1	−26.0 deg
R_{56}	−4.65 cm
A_s	0.305 MV
$n = k_s/k_1$	25
r_1	3.15 mm
r_2	3.50 mm
ϵ	2.8
A_0	2.96 MV/(nC m)
L_{guide}	325 mm

still see that the current distributions do not develop a significant current spike at the bunch head for any of the simulated cases.

B. Case 2: $L_b = 2$ mm, and $C = 6$

If the bunch length is reduced, then the compression factor can be increased as seen from the condition (24). Table III lists the rf and compression parameters for the second-order compensation when the compression factor $C = 6$. In this case the wave number of the linearizer is $k_s = \pi/L_b \approx 1572\ \text{m}^{-1}$. Figure 9 shows the phase space after the magnetic chicane. As in case 1, the phase space remains quite linear and the current distribution does not develop a significant current spike at the head. However, as in case 1 the current distribution displays a distortion due to the fourth-order term if compared with the situation in Fig. 5 when an x-band system is used. In this case the harmonic voltage A_s, calculated from Eq. (20), is approximately 3 times less than the previous case 1 (0.304 MV versus 0.94 MV). Thus, if the bunch length L_b is reduced approximately 40% with respect to case 1, then the linear compression factor can be increased without increasing the nonlinear effects, i.e. $C = 6$. Table III lists the parameters for a possible dielectric-lined waveguide that would meet the requirements necessary to produce the results of Fig. 9. In this case such a dielectric-lined waveguide would be constructed with the same radius r_2 and dielectric material as in the previous case but it would be 325 mm long, i.e., considerably shorter than in the previous case.

As in the previous case a sensitivity analysis was performed and Fig. 10 plots the relative peak current $\Delta I_{pk}/I_{pk}$, relative mean energy $\Delta E/E$, and bunch arrival time variation Δt_f after bunch compression as a function of the bunch length variations $\Delta L_b/L_b$ (upper plots) and the relative charge variations $\Delta Q/Q$ (lower plots) at the injector. As an example, the upper middle plot in Fig. 10

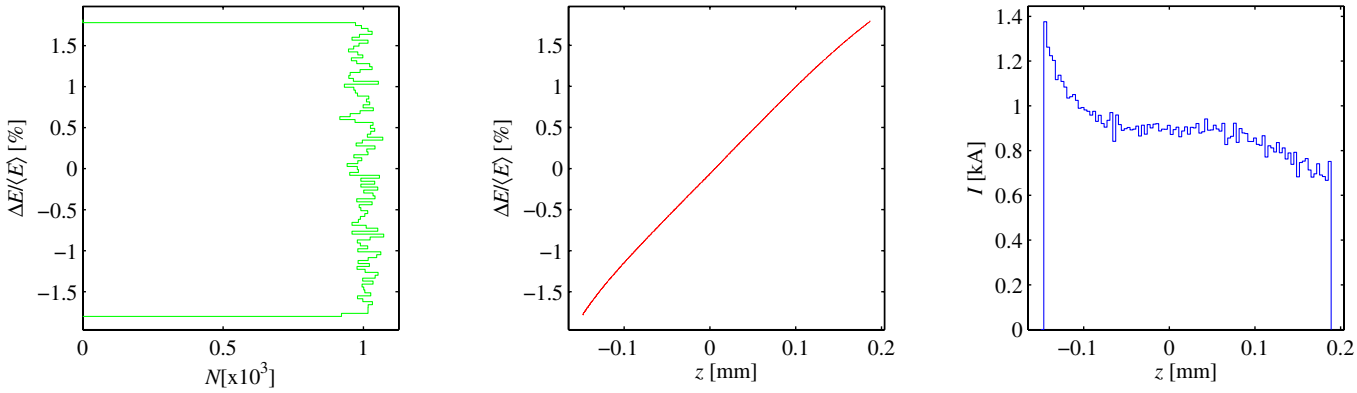

FIG. 9. (Color) Energy profile (left), longitudinal phase space (middle), and bunch current distribution (right) after the bunch compressor when the passive linearizer is used to compensate the quadratic term. The goal is to have a compression factor $C = 6$.

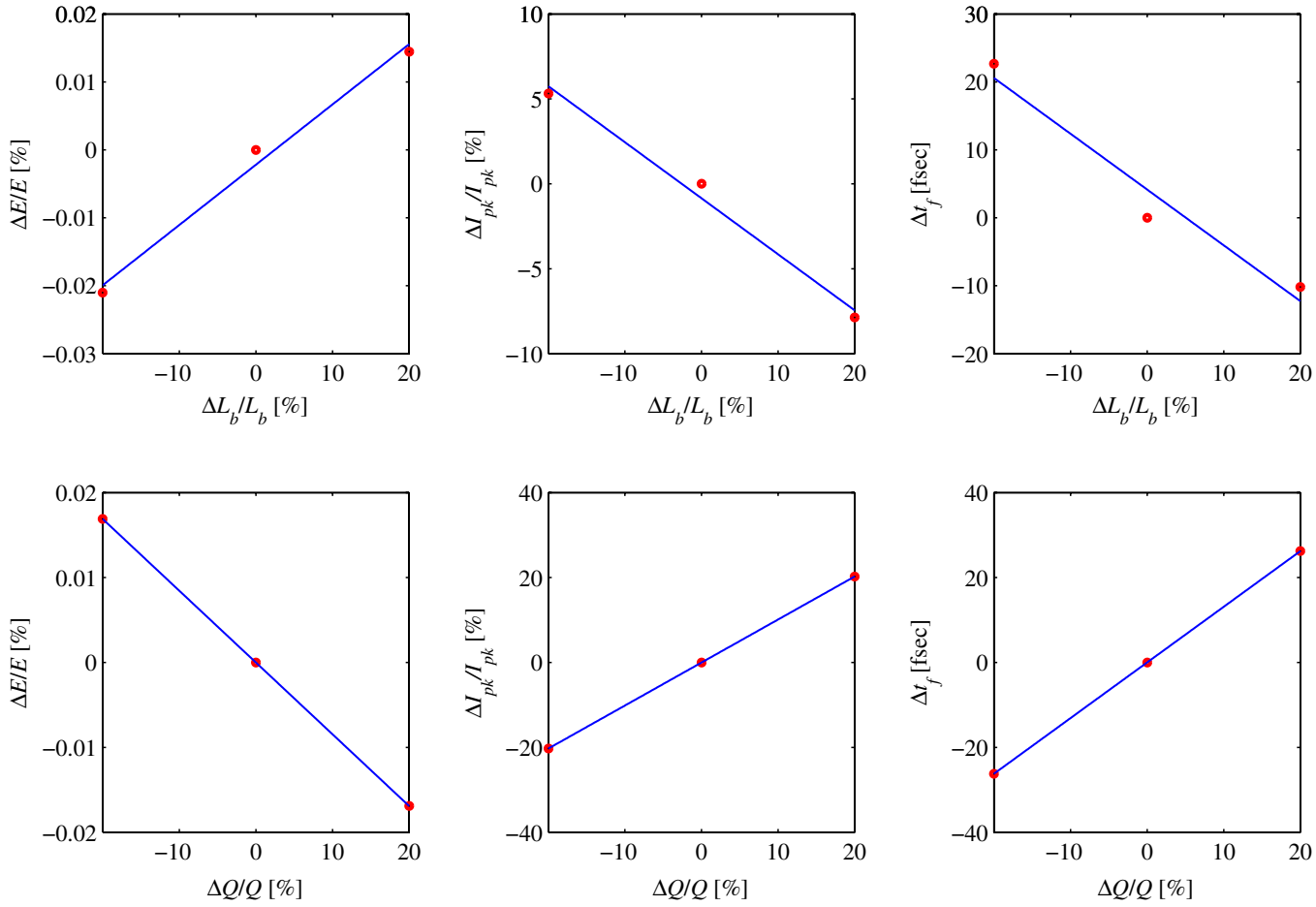

FIG. 10. (Color) Relative mean energy $\Delta E/E$, relative peak current $\Delta I_{pk}/I_{pk}$, and bunch arrival time variation Δt_f as a function of the relative initial bunch length variations $\Delta L_b/L_b$ (upper plots) and relative initial bunch charge variations $\Delta Q/Q$ (lower plots).

indicates that a $\pm 20\%$ bunch length variation at the injector causes an approximately 5% to -8% relative peak current variation after bunch compression. Table IV lists the sensitivities of the electron beam parameters to the relative bunch length and charge variations. As before each sensitivity number quoted in the table independently causes an 8% relative peak current increase, or a 0.1% relative mean energy increase, or a 150 fs bunch arrival time increase. Figure 11 shows the bunch current distributions after the bunch compression chicane for different bunch length variations at the injector and for different relative bunch charge variations. The current distributions do not develop a significant sharp current spike at the bunch head in any cases studied.

V. RAMPED BUNCH DISTRIBUTION

The operation of x-ray free electron lasers (FELs) relies on extremely high quality electron beams. In the presence of wakefields, the electron density distribution plays an important role in the formation of the electron bunch distribution at the end of the accelerator. The electron density distribution with a linear ramped peak current, obtained through a quadratic ramp in the laser intensity, can in principle compensate the nonlinear time dependent variations due to the linac structural wakefields [6]. For this reason we consider a linear ramped charge distribution that can be defined as

TABLE IV. Individual sensitivities. Each parameter variation causes a $\Delta I_{pk}/I_{pk} = +8\%$ relative peak current change, or a $\Delta E/E_0 = +0.1\%$ relative energy change, or a $\Delta t_f = 150$ fs bunch arrival time change after the bunch compression.

Parameters	$\Delta I_{pk}/I_{pk} = +8\%$	$\Delta E/E = +0.1\%$	$\Delta t_f = +150$ fs
$\Delta L_b/L_b$ [%]	-20	>20	< -20
$\Delta Q/Q$ [%]	8	< -20	>20

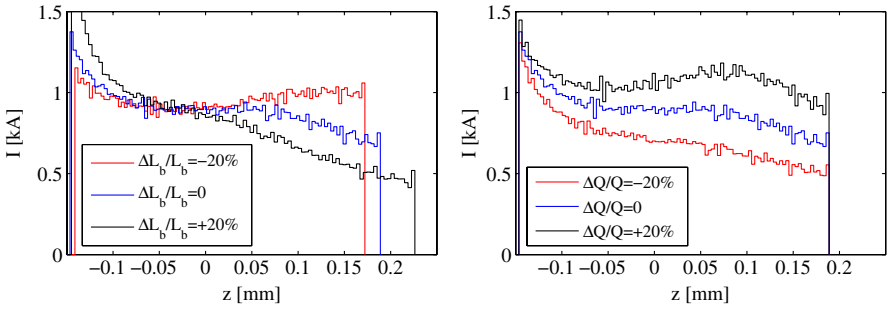

FIG. 11. (Color) Bunch current distributions after the chicane for different bunch length variations at the injector (left plot) and for different relative bunch charge variations (right plot).

$$\rho_{\mathrm{ramp}}(z) = \frac{2}{L_b^2} z + \frac{1}{L_b} \quad \text{if } |z| \le \frac{L_b}{2}. \tag{25}$$

The energy change within the bunch itself in a dielectric-lined vacuum chamber of length L is given by

$$\Delta E_s(z) = -A_s[1 - \cos(k_s z + \phi_s)] \quad \text{if } |z| \le \frac{L_b}{2}, \tag{26}$$

where $A_s = 2QLA_0/k_s^2 L_b^2$ and $\phi_s = (k_s L_b)/2$. In this case the synchronous mode can provide a decelerating voltage at the bunch center when its phase is $\phi_s \sim \pi$ and this condition can be obtained by choosing a dielectric-lined waveguide with $k_s \sim 2\pi/L_b$. The energy change in Eq. (26) can be written as

$$\Delta E_s(z) \approx -A_s[1 + \cos(k_s z)] \quad \text{if } |z| \le \frac{L_b}{2}. \tag{27}$$

As in Sec. III for the rectangular bunch distribution, we can calculate the amplitude A_s of the voltage needed to completely cancel the second-order compression terms:

$$eA_s \approx \frac{E_0(1 + \frac{3a^2}{k_1^2}) - E_i}{(\frac{k_s}{k_1})^2 - 2}. \tag{28}$$

If $k_s \gg k_1$ then the amplitude A_0 of the synchronous mode can be written

$$A_0 \approx \frac{L_b^2}{2} \frac{k_1^2 A_{s0}}{QL}, \tag{29}$$

where A_{s0} is given in Eq. (22). Following the same consideration as in the rectangular bunch distribution, the residual nonlinear effects are small if the following condition holds:

$$\left| \frac{R_{56}}{1 + aR_{56}} \right| \ll \frac{48E_0}{\pi^2 k_1^2 e A_{s0} L_b}. \tag{30}$$

Here we have assumed $k_s L_b \sim 2\pi$ and $k_s \gg k_1$. If we compare the conditions described by Eqs. (24) and (30), then we observe that the conditions required to achieve a similar level of the beam quality as for the rectangular beam case are 4 times more stringent.

VI. TRACKING RESULTS USING A PASSIVE LINEARIZER AND FOURTH-HARMONIC SYSTEM

From the previous sections we have seen that the passive linearizer could work well with a ramped current distribution if the needed harmonic voltage is not too high. An idea could be to use the passive linearizer together with an active fourth-harmonic system for the linearization of the longitudinal phase space. A possible advantage of this option is that both needed voltages, passive and active, could be reduced. In this section we present the tracking results when both systems are used in the one-stage compression option of the FERMI@Elettra project [4]. This option foresees a ramped current distribution with total charge $Q = 0.8$ nC. The single bunch beam is produced by a photoinjector, then accelerated up to 250 MeV and compressed with a single magnetic chicane. After the compression the beam is still accelerated approximately to 1.1 GeV (linac end) by a linear accelerator, and finally transported to the undulators, where the free electron lasing occurs. Figure 12 shows the simulated energy profile, longitudinal phase space, and bunch current distribution at the linac end with parameters given in [4] and using only the fourth-harmonic rf system to compensate the nonlinearities. In this case the required fourth-harmonic voltage is 19 MV with an rf phase of $-195°$. Figure 13 shows the simulated energy profile, longitudinal phase space, and bunch current distribution at the linac end using a combined passive and active system. In this case the fourth-harmonic voltage is 8.5 MV and the synchronous mode has an amplitude of 4.4 MV/(nC m) and a wave number $k_s = 1440\ \mathrm{m}^{-1}$. Assuming the fourth-harmonic accelerating structure presented in [7], we need an rf power of 4.2 MW if we use the passive linearizer, and 21 MW if we only use the fourth-harmonic system. This becomes a practical issue as x-band rf power systems below 5 MW are commercially available, but at present above that value they are not.

The required voltage for the passive linearizer and the relative wave number can be reached with one dielectric-lined waveguide 1-m long with radii $r_1 = 2.4$ mm and

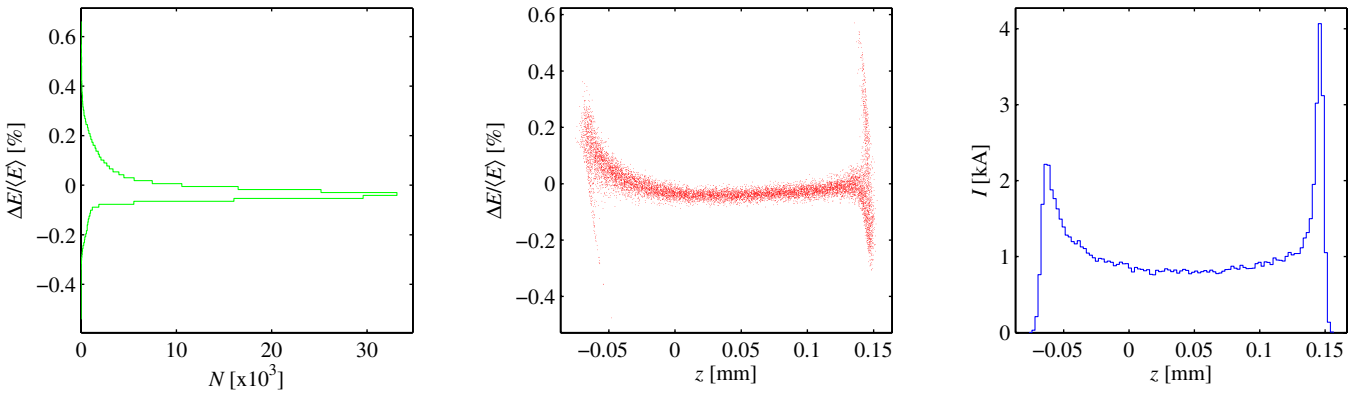

FIG. 12. (Color) Energy profile (left), longitudinal phase space (middle), and bunch current distribution (right) at the linac end when the one-stage compression option as described in [4] is considered. Bunch mean energy $\langle E \rangle = 1067$ MeV.

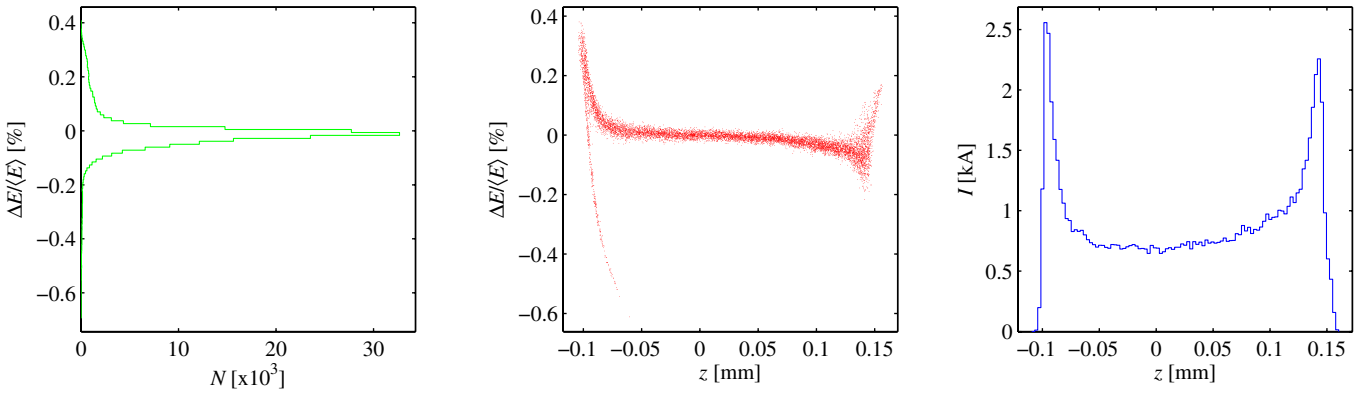

FIG. 13. (Color) Energy profile (left), longitudinal phase space (middle), and bunch current distribution (right) at the linac end when the combined option, passive and active linearizer, is considered. Bunch mean energy $\langle E \rangle = 1076$ MeV.

$r_2 = 3$ mm. The dielectric material should have a relative dielectric constant $\epsilon = 2.2$ with a thickness of 0.6 mm. The second characteristic wave of the waveguide has the following parameters: $A_1 = 0.5$ MV/(nC m) and $k_{s1} = 5300$ m^{-1}. Figure 14 shows the simulated energy profile, longitudinal phase space, and bunch current distribution at the linac end considering also the second characteristic wave. In such a case the fourth-harmonic voltage is 9 MV and the rf phase $-200°$. This is needed to compensate the spurious effect due to the second characteristic wave.

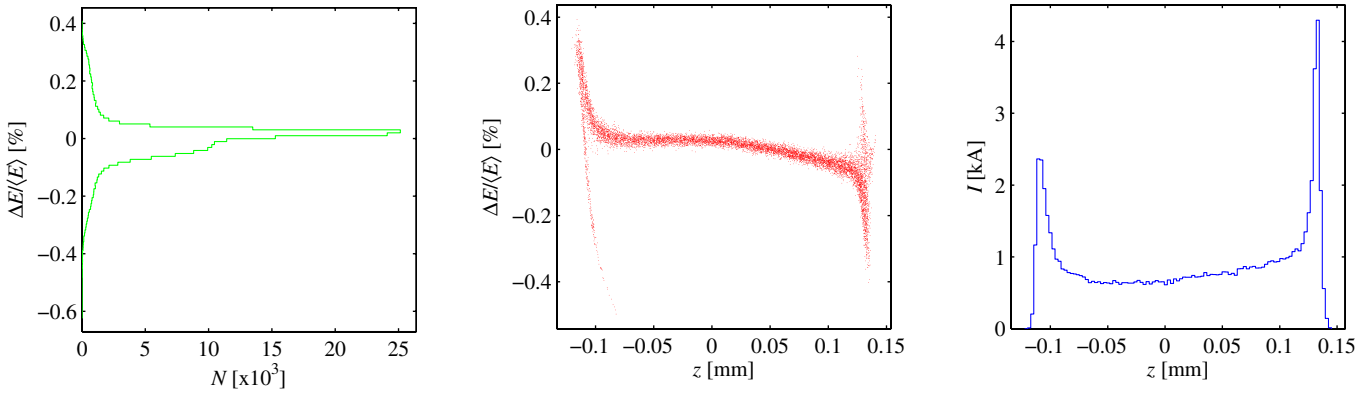

FIG. 14. (Color) Energy profile (left), longitudinal phase space (middle), and bunch current distribution (right) at the linac end when the combined option, passive and active linearizer, is considered. For the passive linearizer the second characteristic wave is also considered. Bunch mean energy $\langle E \rangle = 1076$ MeV.

VII. CONCLUSION

In this paper a passive linearizer is implemented instead of an active fourth-harmonic linearizer system to compensate both for the second-order rf time curvature and for the second-order momentum compaction terms. Using the passive linearizer, the current distribution does not develop a significant sharp peak current spike at the head of the beam. On the other hand, there is a distortion of the current distribution due to the fourth-order term introduced by the convolution between the wake function of the dielectric-lined waveguide and the charge distribution. A condition to limit the nonlinear effects due to the fourth-order term is given. Basically, there are two possibilities in keeping the spurious effects small: the first one is to reduce the bunch length from the photoinjector and the second one is to use a small linear compression factor. We have presented the LITRACK tracking results considering two cases of a rectangular bunch distribution with different bunch length and different linear compression factors. For both cases the results have shown that the linearizer can be successfully used in place of the active fourth-harmonic system. Since the energy change within the bunch due to passage through the dielectric-lined waveguide strongly depends on the bunch distribution and charge, we have carried out a sensitivity study for both the case of charge variations and for variations in bunch length of the considered bunch distributions. We have seen that the current distributions do not develop a significant sharp peak current spike at the bunch head for any of the simulated cases. On the other hand, the linearizer is, however, tailored to a particular bunch charge and current distribution. In this case in order to accommodate a range of bunch charges and current distributions, a possible idea is to implement the passive linearizer involving multiple waveguides with separate properties on a movable stage. Each of the dielectric-lined waveguides tailored would be tailored with a different wave number k_s and amplitude A_0. Furthermore, the results for the linear ramped bunch distribution, such as that used in [1], were presented. Finally, we have successfully studied the passive linearizer together with an active fourth-harmonic system for the one-stage compression option of the FERMI@Elettra project. As a conclusion, the linearizer can, in principle, be used instead of an active higher harmonic system if the compression factor or the bunch length from the photoinjector is limited. In addition, another result from this work is the suggestion to use the passive linearizer together with an active higher harmonic system. In this way the required higher harmonic voltage could be reduced.

As a final point we must consider the transverse wakefields that can be generated in the dielectric-lined waveguide. The wake functions can be calculated as shown in [3]. For the passive linearizers proposed in this paper, the amplitude of the transverse wake functions are of the same order of magnitude, approximately a factor 2–3 larger when compared to the active fourth-harmonic cavity foreseen for the FERMI layout. Thus, in principle, the transverse wake effects due to the passive linearizer may result in a limited but acceptable amount of emittance growth.

ACKNOWLEDGMENTS

We thank Stephen Milton for the careful review of this paper and Giuseppe Penco and Simone Di Mitri for helpful discussions and suggestions.

[1] For example, see C. J. Bocchetta *et al.*, FERMI@Elettra Conceptual Design Report No. ST/F-TN-07/12, 2007.
[2] P. Emma, Technical Note No. LCLS-TN-01-1, 2001.
[3] K. Y. Ng, Phys. Rev. D **42**, 1819 (1990).
[4] M. Cornacchia *et al.*, FERMI Report No. ST/F-TN-07/08, 2007.
[5] K. L. F. Bane and P. Emma, in *Proceedings of the 21st Particle Accelerator Conference, Knoxville, 2005* (IEEE, Piscataway, NJ, 2005).
[6] M. Cornacchia *et al.*, Phys. Rev. ST Accel. Beams **9**, 120701 (2006).
[7] P. McIntosh *et al.*, in Proceedings of the 21st Particle Accelerator Conference, Knoxville, 2005 (Ref. [5]).